Journal of Food Engineering 92 (2009) 8–17

Contents lists available at ScienceDirect

Journal of Food Engineering

journal homepage: www.elsevier.com/locate/jfoodeng

Experimental determination and modelling of size variation, heat transfer and quality indexes during mushroom blanching

A.R. Lespinard [a], S.M. Goñi [a,b,c], P.R. Salgado [a], R.H. Mascheroni [a,c,*]

[a] Centro de Investigación y Desarrollo en Criotecnología de Alimentos (CIDCA), CCT La Plata CONICET – Facultad de Ciencias Exactas, UNLP, 47 y 116, B1900AJJ La Plata, Buenos Aires, Argentina
[b] Departamento de Ciencia y Tecnología, UNQ, Bernal, Argentina
[c] MODIAL – Depto. Ing. Química – Facultad de Ingeniería, UNLP, La Plata, Argentina

ARTICLE INFO

Article history:
Received 12 March 2008
Received in revised form 14 October 2008
Accepted 16 October 2008
Available online 5 November 2008

Keywords:
Blanching
Mushroom
Heat transfer
Volume contraction
Finite elements
Colour
Texture
Polyphenoloxidase

ABSTRACT

Process time during mushrooms blanching is determined either by shrinking rate or by polyphenoloxidase (PPO) inactivation, depending on the value of heating bath temperature. Quality losses during blanching can be minimized through an adequate selection of the time–temperature schedule. In this work shrinkage and PPO enzymatic activity of mushroom during blanching were measured. A simple kinetics of mushroom shrinkage was developed and was coupled to a heat transfer model based on the finite element method with irregular domain. The effect of this process on the textural and colour quality was experimentally studied and compared with the cooking value predicted from temperature simulations. Shrinkage was found to be the limiting factor to estimate the processing time for bath temperature higher than 60 °C; while polyphenoloxidase activity reduction was the limiting factor at lower bath temperatures. Quality indexes diminished with thermal treatment. Texture measures were in good agreement with simulated cooking values. This last parameter can be optimized by selecting the most appropriate conditions for the blanching process.

1. Introduction

Edible fungi, like mushrooms, have been used as food since ancient times. At least 25 species of fungi have been considered as edible food, but few of them have reached commercial significance. Mushrooms (*Agaricus bisporus*) are one of the most popular and valuable of these edible fungi and are they usually processed for a long-time storage. Mushrooms are highly perishable commodities due to their large content in nutrients (they have – in average – 3.27% crude protein, 0.24% crude fat and 4.77% total carbohydrate on a wet basis) and their high respiration rate, factors that induce deterioration immediately after harvest (Kotwaliwale et al., 2007). Browning reactions limit their shelf life to a few days, being the enzyme polyphenoloxidase (PPO, monophenol, dihydroxy-L-phenylalanine) the main responsible for this deteriorative process. In view of their highly perishable nature, mushrooms must be processed to extend their commercial shelf life for off-season use (Devece et al., 1999).

The production of heat-sterilized preserves represents most usual long-term preservation. Sterilization accounts for more than 60% of industrial processed mushrooms. In the preparation process of sterilized mushrooms, blanching is an important pre-treatment, which objectives may be: (i) to reduce enzymatic browning through thermal inactivation of PPO; (ii) to induce volume contraction (shrinkage) in order to avoid this occurrence at the sterilization stage; (iii) to make the product more pliable to facilitate filling operations (Biekman et al., 1996). However, some negative features of blanching are the extraction of valuable nutritious components, partial biochemical conversions of components resulting in changes in aroma and – in general – deteriorative effects on sensory properties like texture and colour (Matser et al., 2000), which are the main features taken into account by consumers (Kotwaliwale et al., 2007).

Volume change and the rate of heat transfer, together with deteriorative reactions, are the main features to be taken into account during the design and optimization of sterilization procedures for mushrooms. Available literature presents few references on modelling of volume contraction and heat transfer during the sterilization of mushrooms. McArdle and Curwen (1962) have shown that most of shrinkage (up to 25%) occurs during blanching, and that the whole process (blanching plus sterilization) involves weight loss within the range of 30% to 40%. Konanayakam and Sastry (1988)

* Corresponding author. Address: Centro de Investigación y Desarrollo en Criotecnología de Alimentos (CIDCA), CCT La Plata CONICET – Facultad de Ciencias Exactas, UNLP, 47 y 116, B1900AJJ La Plata, Buenos Aires, Argentina. Tel./fax: +54 221 425 4853.
E-mail address: rhmasche@ing.unlp.edu.ar (R.H. Mascheroni).

0260-8774/$ - see front matter © 2008 Published by Elsevier Ltd.
doi:10.1016/j.jfoodeng.2008.10.025

Nomenclature

A	button (cap) diameter (m)
A_1	pre-exponential factor (s^{-1})
C	cooking value (min)
C_p	specific heat capacity of mushroom ($J\ kg^{-1}\ K^{-1}$)
d	stem diameter (m)
DO	optical density (at 410 nm)
D	characteristic dimension (m)
D_{rave}	average absolute relative difference between simulated and experimental temperatures (%)
E_a	Arrhenius activation energy ($kJ\ mol^{-1}$)
h	convective heat transfer coefficient ($W\ m^{-2}\ K^{-1}$)
H	button (cap) height (m)
k	thermal conductivity ($W\ m^{-1}\ K^{-1}$)
K_1	rate constant of change of characteristic dimension (A or L) (s^{-1})
K_m	average rate constant of change of characteristic dimension (s^{-1})
L	length of mushrooms (m)
m	number of experimental values
R^2	determination coefficient
R	universal gas constant ($J\ K^{-1}\ mol^{-1}$)
t	time (min)
T	temperature (°C or K)
$T(x, y, z, t)$	temperature at given co-ordinates and time (°C)
T_∞	heating medium temperature (°C)
V	volume of mushroom (m^3)
x, y, z	space coordinates (m)
z_c	thermal resistance factor for nutritious components (°C)
ρ	density ($kg\ m^{-3}$)
Γ	mushroom surface
Ω	mushroom domain

Subscripts

ave	average
e	experimental
eq	equilibrium
f	final
0	initial
r	relative
ref	reference
S	simulated
sur	surface
t	at time *t*

described mass and volume shrinkage, for vacuum-hydrated mushrooms, using three successive first order kinetics, their number (two or three phases) and duration depended on water-bath temperatures. Normally, during heating, there is an initial stage of slow-rate shrinkage that is only evident at low bath temperatures, followed by a fast-rate shrinkage period. Shrinkage is finished at another slow-rate stage.

Sheen and Hayakawa (1991) developed a simulation model for the temperature change during freezing and thawing of mushrooms with phase and volumetric changes. Biekman et al. (1997) used an empirical approach to link shrinkage to heat transfer in mushrooms during blanching, showing that their rates are related to water-bath temperature and mushroom size and that the effects on contraction and heat transfer are synergistically linked. Sensoy and Sastry (2004) studied blanching of de-stemmed mushroom caps heated in boiling water or with ohmic heating, determining volume change and heat transfer. In the above mentioned works neither shrinkage nor heat transfer were related to quality parameters. The final objective of this work was to characterize mushroom blanching and the changes in quality indexes produced during this process. To this aim, specific objectives were: (1) to develop a simple size change kinetics and to measure PPO activity, so as to determine limiting factors to blanching process; (2) to model heat transfer through the mushroom; (3) to evaluate changes in colour and texture and their correlation with simulated cooking values.

2. Materials and methods

2.1. Samples

Freshly harvested mushrooms (*A. bisporus*) were bought at a local market, kept in refrigerated storage at 4 °C, and then used for the experimental tests within 24 h.

2.2. Thermal treatments

Mushrooms were selected according to size and gently washed with water at room temperature to remove foreign materials that could be adhered to their surface. Samples were grasped in a stand and submerged into the thermostatized water bath (HAAKE F3, Germany) according to the procedure described in Section 2.3. Equivalent blanching processes were designed, at different water-bath temperatures (50, 60, 70, 80 and 90 °C), so as to obtain the same size shrinkage of the product. In each test, process times were estimated in order to reach a size contraction of 18% (80% of the highest size reduction). When the estimated process times were reached, samples were removed from the heating bath and immediately sunk in a water-ice mixture for 2 min.

2.3. Image acquisition and size determination

A computer vision system (CVS) that is a digital camera (Professional Series Network IP Camera, Intellinet Active Networking) coupled to a PC (AMD Sempron 2200, 768 MB-RAM), was used. The digital camera was assembled by means of a stand that is perpendicular to the thermostatized bath (Fig. 1).

Samples were grasped to another stand built to hold up to 12 samples, which colour contrasted with that of the samples in order to increase image definition by the CVS. Using this procedure, samples remained fixed inside the bath and image acquisition could be optimally performed without moving the camera. Samples were placed vertically and horizontally to determine height and diameter variation. A reference object, a piece of white plastic material (4 cm × 4 cm cross section), was also immobilized on the stand and used as size pattern.

Mushroom images were taken during blanching, at 30-second intervals at the first stage, and every 120 s at the final stage of the process. Image acquisition was stopped when no size variation in samples was detected. Later, image processing was performed on the recorded images to estimate the characteristic dimensions of samples (L and A) and their variation with process time (see Fig. 2).

In this regard, *Image Processing Toolbox*, MATLAB (MathWorks, Natick, Massachusetts), was used according with the following steps (Goñi et al., 2007):

- Conversion of original RGB images to grey-scale format.
- Noise reduction through a 3 × 3 median filter to enhance image quality.

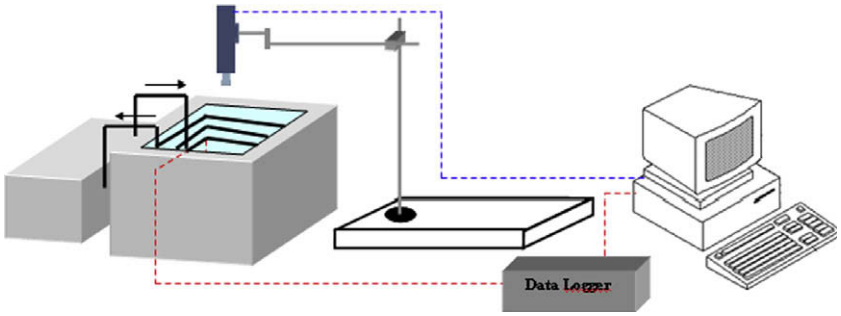

Fig. 1. Scheme of the thermostatized water bath and of the computer vision system.

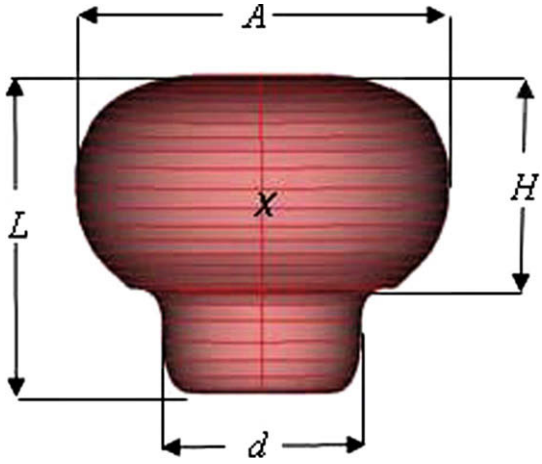

Fig. 2. Mushroom geometry showing the characteristic dimensions and the location (X) of the thermocouple for temperature determination.

- Segmentation through a threshold value which was obtained by analyzing the grey-scale image histogram. A binary image was obtained where black colour (pixel value equal to 0) represented the background and white colour the sample (pixel value equal to 1).
- Width and height of the binary images of samples (in pixels) were measured. A conversion factor, computed from the reference object, was used to convert the mushroom dimensions from pixels to SI units. Also, the characteristic dimensions of three samples (*A, L, H* and *d*) were measured with a Vernier caliper before and after blanching; they were also used to validate the ones obtained by the CVS.

The experimental variation of A and L with time, in dimensionless shape, was adjusted to an exponential model (Eq. (1)), where D_t is the instantaneous value of the characteristic dimension (A or L) at a time t (min); D_0 is its initial value; D_{eq} the equilibrium dimension (after a long blanching time) and K_1 is the temperature-dependent rate constant. The temperature dependence was modelled through an Arrhenius-type relationship (Eq. (2)), where A_1 is the pre-exponential factor (s^{-1}), E_a is the activation energy (J mol^{-1}), R is the universal gas constant (8.31 J mol^{-1} K^{-1}), and T is water bath temperature (K). The pre-exponential factor and the activation energy can be determined by linear regression of $log\ (K_1)$ vs. $1/T$, being $-E_a/R$ the slope and $log\ (A_1)$ the ordinate at origin.

$$\frac{D_t - D_{eq}}{D_0 - D_{eq}} = \exp(-K_1 * t) \tag{1}$$

$$K_1 = A_1 * \exp\left(\frac{-E_a}{RT}\right) \tag{2}$$

2.4. Reconstruction of mushroom shape

Three-dimensional mushroom shapes were built from images of transversal cuts of samples (Fig. 3a). These images were digitally processed to obtain a binary image, as previously described (Fig. 3b), whose contour was approximated with a *B–Spline* curve (Fig. 3c), which was used as a base for the construction of the simulation domain. To construct the axisymmetric two-dimensional domain, the *B–Spline* curve was transformed into a solid object. The three-dimensional domain (Fig. 3d) was obtained by revolution of the axisymmetric two-dimensional domain.

2.5. Temperature acquisition

In other series of experiments, the same test conditions as described in Section 2.2 were repeated and temperatures in the water bath and in the thermal centre of the mushroom (geometric centre of mushroom head) (Fig. 2) were measured every 15 s using rigid type T thermocouples (copper–constantan (Cu–CuNi), OMEGA, USA). Thermal histories were recorded using a multi-channel data acquisition system (KEITHLEY model AS-TC, USA).

2.6. Modelling of heat penetration

A mathematical model was developed to describe conduction heat transfer through the vegetable (Eq. (3)), with uniform initial temperature (Eq. (4)) and convective boundary conditions (Eq. (5)).

$$\rho C_p \frac{\delta T}{\delta t} = \nabla(k \nabla T) \tag{3}$$

$$T(x, y, z, t = 0) = T_0 \tag{4}$$

$$k \nabla T = h(T_\infty - T) \tag{5}$$

Shrinkage was coupled to the heat transfer model through Eq. (1) using an arbitrary Lagrangian–Eulerian method (COMSOL AB, 2005). The boundary condition for shrinkage was computed through the velocity of the geometric boundaries obtained from time derivative of the characteristic dimension (Eq. (6)).

$$vel_D = \frac{dD_t}{dt} = -K_1(D_0 - D_{eq}) \exp(-K_1 * t) \tag{6}$$

where vel_D is the velocity of size change in the D characteristic dimension direction.

The moving boundary displacement was then propagated throughout the domain obtaining a smooth mesh deformation over all the sample volume (COMSOL AB, 2005).

To run the finite element model the volume dominium (mushroom) was discretized by means of a grid of simplices (distorted tetrahedrons) that can approximate to the boundary better than the ordinary, straight mesh elements (COMSOL AB, 2005) (Fig. 4). The following constant thermophysical properties were used: C_p = 3883 J kg^{-1} K^{-1}, k = 0.4324 W m^{-1} K^{-1} (Sastry et al., 1985).

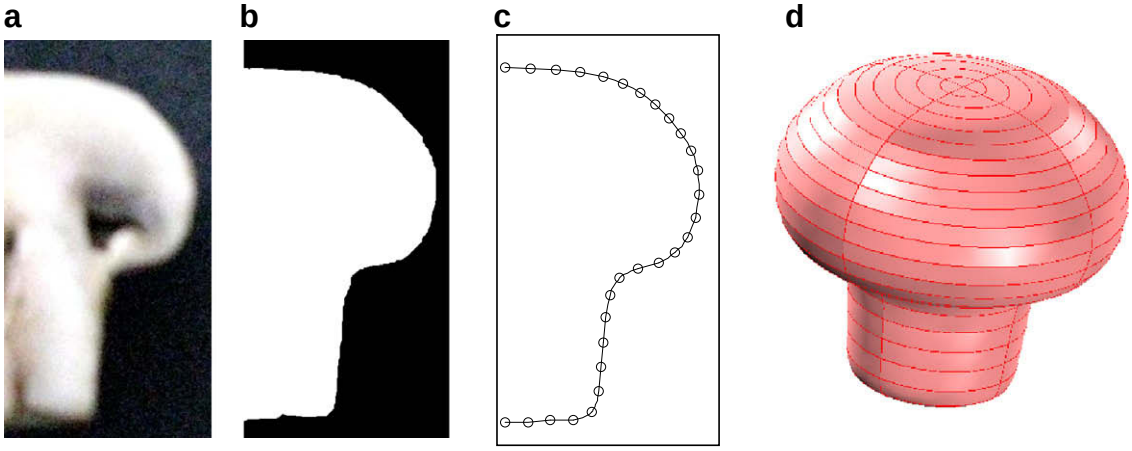

Fig. 3. Sequence of the development of mushroom shape. (a) image of a transversal cut; (b) binary image; (c) *B-Spline* curve; (d) revolution solid.

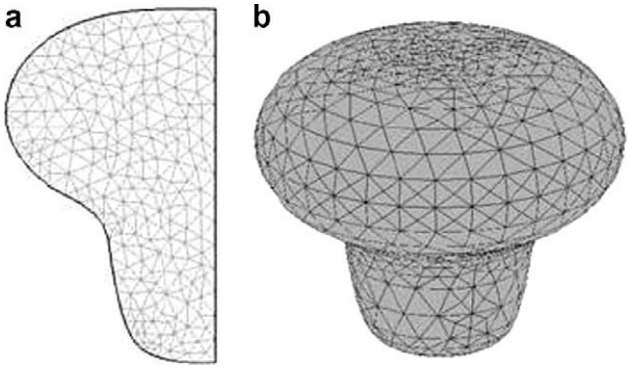

Fig. 4. Computational meshing of the mushroom. (a) 2D axisymmetric geometry, 341 triangles; (b) 3D geometry, 8508 tetrahedrons.

Mushroom density was determined from weight and volume measurement of a sample lot –liquid displacement method–, and was found to be 689.6 kg m^{-3}.

To estimate the heat transfer coefficient a bronze mushroom shaped object was manufactured. Bronze was chosen as a test material due to its high thermal diffusivity, which assures an almost instantaneous uniform temperature profile. A thermocouple was inserted at the centre of object to sense the time–temperature history and the thermal treatments described in Section 2.2 were carried out in the same water bath system. The temperature of the thermal centre was plotted in a semi-logarithmic scale and the heat transfer coefficient was calculated from the slope of the linear response obtained, assuming a lumped parameter behaviour. The following thermophysical properties for bronze were used: $\rho = 8470$ kg m^{-3}, $C_p = 376.81$ J kg^{-1} K^{-1}, $k = 122.87$ W m^{-1} K^{-1}. The surface area and volume for calculations were estimated from a geometric model of the object, which was created using a digital image of the object. Heat transfer coefficient was found to linearly vary with water bath temperature, and the following values were obtained: 645.47, 782.54, 815.76, 916.50 and 1072.60 W m^{-2} K^{-1}, for water bath temperatures of 50, 60, 70, 80 and 90 °C, respectively.

2.7. Model validation

The heat transfer model was validated by comparing experimental and simulated mushroom temperatures. These comparisons were performed calculating the average relative differences D_{rave} (Eq. (7)):

$$D_{rave} = \frac{100}{m}\sum_{i=1}^{m}\left\|\frac{Ts - T_e}{T_e}\right\| \tag{7}$$

3. Evaluation of quality indexes

3.1. Cooking value

Both, the average cooking value (C_{ave}) and the surface cooking value (C_{sur}), were determined by numerical integration of Eqs. (8) and (9), respectively, using the simulated temperature profiles for each sample. A reference temperature (T_{ref}) of 100 °C and a z_c value of 23 °C were considered for calculations. The value of z_c was chosen as the average of those values corresponding to the deterioration kinetics of sensory quality parameters (Ohlsson, 1980).

$$C_{ave} = \int_0^{t_f}\left(\frac{\int_\Omega 10^{\frac{T(t,\Omega)-T_{ref}}{z_c}}\partial\Omega}{\int_\Omega \partial\Omega}\right)\partial t \tag{8}$$

$$C_{sur} = \int_0^{t_f}\left(\frac{\int_\Gamma 10^{\frac{T(t,\Gamma)-T_{ref}}{z_c}}\partial\Gamma}{\int_\Gamma \partial\Gamma}\right)\partial t \tag{9}$$

3.2. Determination of texture

Firmness of fungi was measured with a texturometer TA-XT2i (Stable Micro Systems Ltd., Godalming, Surrey, UK) and data were recorded and processed with the Texture Expert Exceed software.

After cutting the tail of mushrooms, their heads were compressed with a cylindrical probe, 10 mm in diameter. Texture analysis was carried out under the following instrument parameters: pre-test speed 10 mm/s; test speed 5 mm/s; post-test speed 5 mm/s; strain 30% of sample height; trigger force 0.05 N; data acquisition rate 25 pps.

Each reported value corresponded to the mean of seven measurements, for unprocessed as well as processed samples. Results were presented as relative percent variation with respect to the initial (unprocessed) sample.

3.3. Determination of colour

Colour determination was carried out using a Minolta colorimeter CR 300 Series (Osaka, Japan) with a measuring area of 8 mm diameter. The instrument was calibrated with a standard white plate ($Y = 93.2$, $x = 0.3133$, $y = 0.3192$). The colour of mushrooms

was measured by L^*, a^* and b^* chromaticity co-ordinates of the CIE-Lab scale (CIE, 1978).

Parameters L^*, a^* and b^* were determined for seven unprocessed and seven processed samples, for each heating condition. Measurements of each sample were performed in triplicate and averaged. Results were presented as relative percent variation with respect to the initial (unprocessed) sample.

3.4. Enzymatic activity of polyphenoloxidase

For the extraction of enzyme PPO the protocol described by Concellón (2003) with small modifications was followed. The samples (fresh or processed fungi) were frozen with liquid nitrogen and ground in a mixer (De Longhi, KG 30, Italy). Three grams of the sample were homogenized (1 h, 4 °C) with phosphate buffer (KH_2PO_4 0.1 M; Na_2HPO_4 0.1 M; Tritón X-100 0.15 v/v; PVPP 30 g L^{-1}; pH 6), then centrifuged at 11,200*g* at 4 °C (for 15 min) (Beckman Coulter, Avanti J-25, USA). The supernatant was separated to determine the enzymatic activity, using a phosphate buffer with 4-methylcatechol (Sigma, Sigma Chemical Co., USA) as enzymatic substrate (KH_2PO_4 0.1 M; Na_2HPO_4 0.1 M; 4-methylcatechol 0.012 M; pH 6). The reaction was carried out at 30 °C. The appearance of colour compounds resulting from the enzymatic oxidation of 4-metilcatechol was measured using a spectrophotometer (BECKMAN DU650, USA) at 410 nm. The determinations were made in duplicate and the enzymatic activity was expressed as the change in absorbance per minute per gram of fresh weight (DO min^{-1} g^{-1}).

3.5. Statistical analysis

Textural and colour data were subjected to analysis of variance (ANOVA) using software STATGRAPHICS Plus 4.0. (Manugistics Inc., USA). Comparison of means between raw and blanched samples were performed using the Tukey's test, at a significance level $p = 0.05$.

4. Results and discussion

4.1. Size variation

Fig. 5 displays the sequence of images obtained with the CVS and their binary equivalents obtained after processing the original images, for a sample blanched with water bath at a temperature of 90 °C. The images showed a rapid size reduction at the first stages of heating, then it became slower at higher process times, tending to a final constant size.

The values of the rate constants (K_1) obtained for the variation of *A* and *L* were similar in each process, implying almost equal degrees of radial and longitudinal contraction. Thus both constants were averaged, obtaining an overall rate constant (K_m) that represents global shrinkage (Table 1) for each process condition. Calculated values of K_m showed a steady increase with water bath temperature, which means an augmentation of the contraction rate with temperature. From regression analysis, values of 59.37 kJ mol^{-1} and 1.40×10^6 s^{-1} were obtained for E_a and A_1 (respectively) with $R^2 = 0.9953$.

Table 2 shows the average percent reductions reached by the different characteristic dimensions at long process times, after these dimensions had reached their equilibrium value (D_{eq}). These values are in accordance with those reported by McArdle and Curwen (1962), who determined an average size reduction of 25%. From the data in Table 2 it can be observed that the mushroom shrinks in almost equal proportions in the longitudinal and in

Table 1
Averaged rate constants for shrinkage as a function of water bath temperature.

Temperature (°C)	Number of samples	K_m (s^{-1}) × 10^3	S.D. (s^{-1}) × 10^4
50	7	0.33	2.35
60	6	0.69	1.23
70	6	1.07	1.38
80	8	2.18	9.35
90	3	3.88	1.90

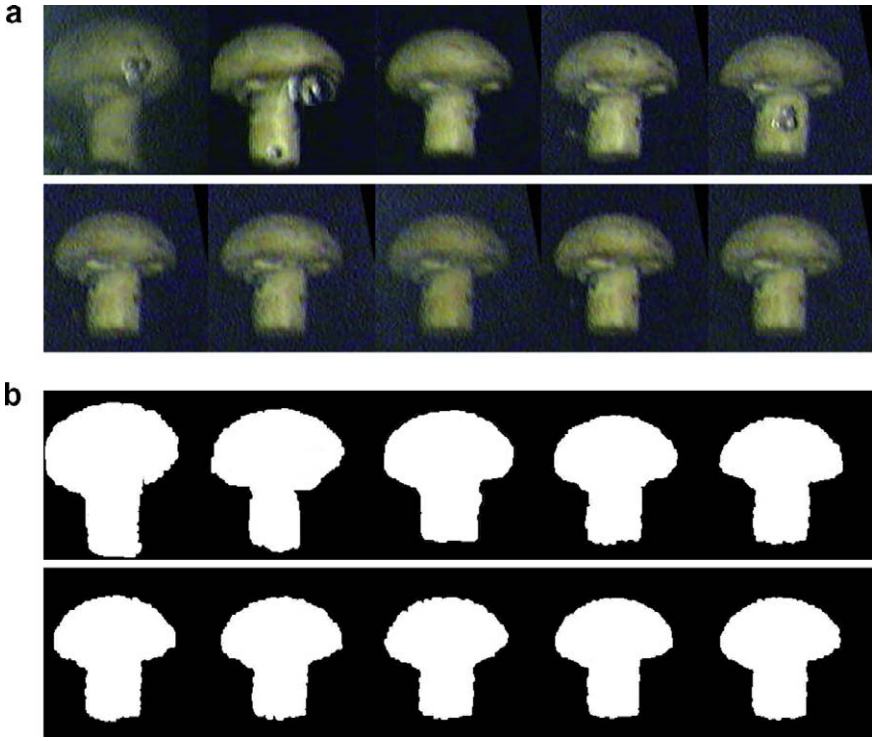

Fig. 5. Images sequence (left to right), every 1 min, showing size variation during blanching at 90 °C, for 9 min. (a) original images, (b) binary (processed) images.

Table 2
Percent reduction of characteristic dimensions at long process times for different bath temperatures.

Temperature (°C)	*A*	*L*	*H*	*d*
50	22.05	23.16	22.05	15.42
60	22.92	22.56	25.22	10.09
70	21.11	22.53	21.94	7.85
80	24.49	26.70	27.30	7.02
90	22.16	27.24	28.57	10.21

the radial directions (21.11–24.49% for *L* against 22.53–26.70% for *A*). On the other hand, stem diameter (*d*) shrinks much less than the other characteristic dimensions. This difference in size reduction can be explained by the fact that the cap has a much less compact structure than the stem, occluding much more air, which can be easily removed during blanching, leading to increase of the contraction process.

Comparing of manual measurements of characteristic dimensions and the ones obtained by the CVS were on good agreement, with relative differences less than 5%.

Fig. 6 shows the predicted variation of the characteristic dimension *A*, simulated by the parameters from the regression model (Table 1). After analyzing the shape of these curves, a size reduction of 18% was found to be a suitable end point for the blanching process. Greater size reductions at this stage led to very long process times at low bath temperatures. Thus blanching times of 77.0,

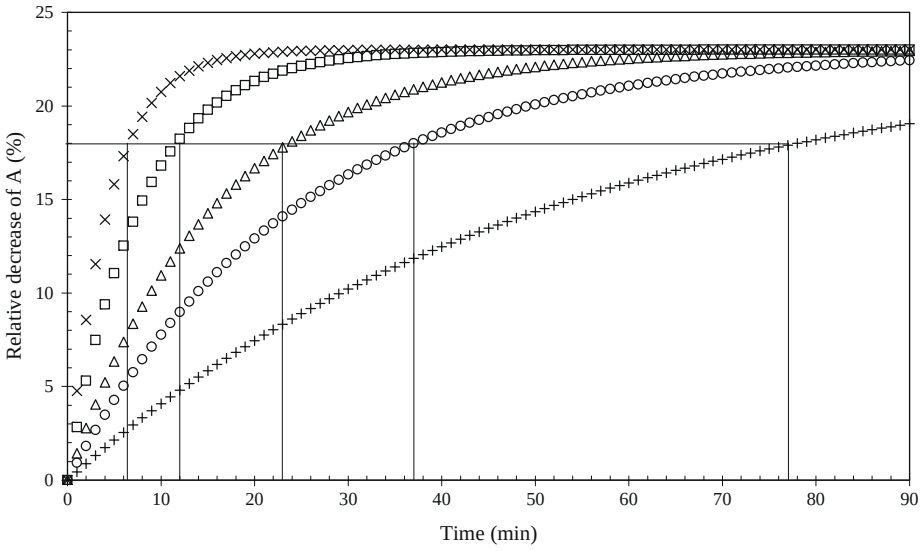

Fig. 6. Predicted variation of the characteristic dimension *A*, using the parameters from the regression model, and estimated process time to reach a reduction of 18%, for different bath temperatures: (x) 90 °C; (□) 80 °C; (Δ) 70 °C; (○) 60 °C; (+) 50 °C.

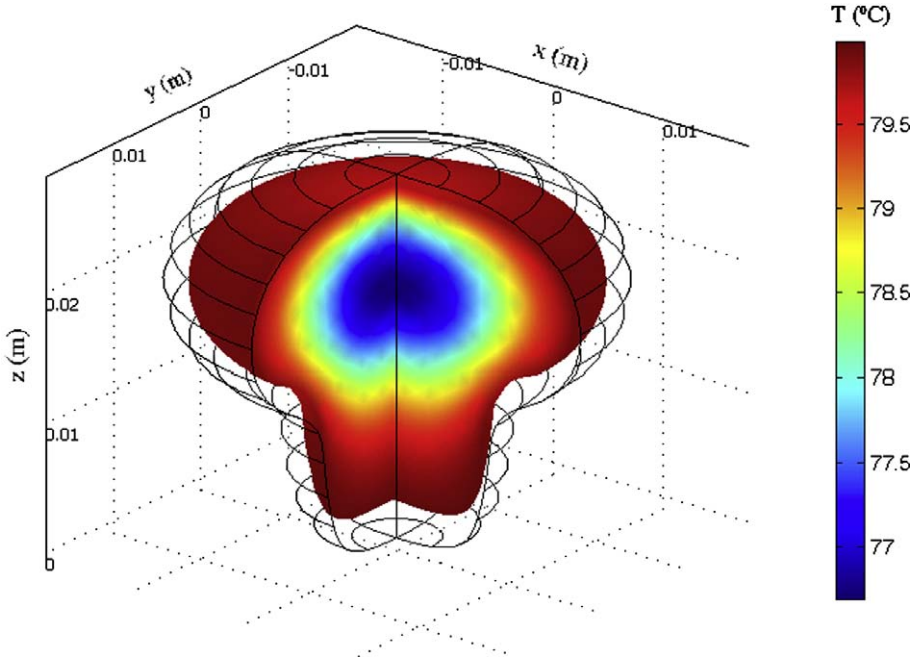

Fig. 7. Predicted surface temperature and size after 6 min of blanching at 80 °C. Solid lines show the initial geometry. (For interpretation to colours in this figure, the reader is referred to the web version of this paper.)

37.0, 23.0, 12.0 and 7.0 min, respectively, were needed for heating bath temperatures of 50, 60, 70, 80 and 90 °C.

4.2. Simulation of temperature profiles

Fig. 7 displays a 3D graph of one mushroom, with predicted surface temperature, after 6.0 min of blanching at 80 °C. The same graph includes the initial and final shapes and sizes of the mushroom. Also, it can be observed that the coldest point coincides with the geometrical centre of the cap and that the stem is the part of the mushroom that reaches the highest temperatures.

As can be seen in Fig. 8, simulated temperatures for the thermal centre, during blanching at 70 °C, showed a high correlation with the experimental ones. Absolute average relative differences lower

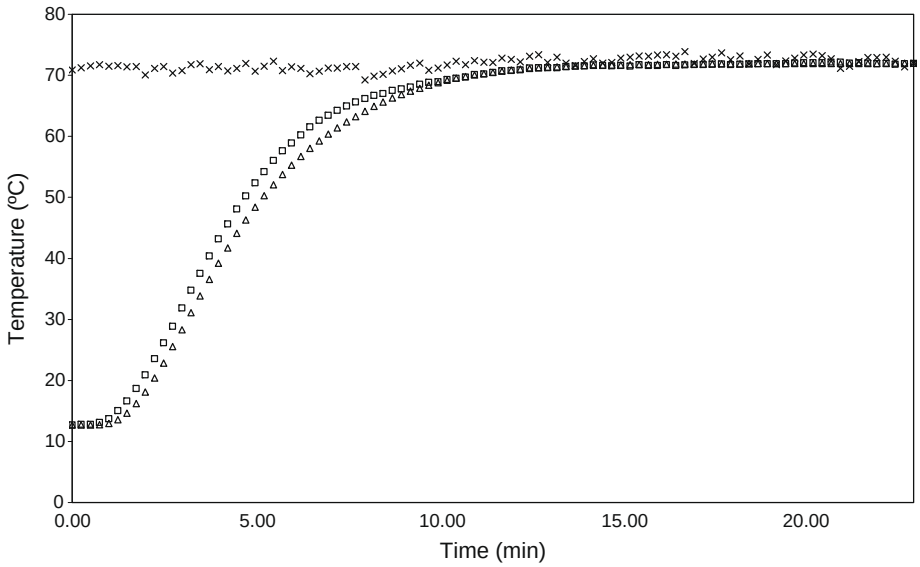

Fig. 8. Temperature evolution during blanching at 70 °C. (□) experimental in the thermal centre; (Δ) simulated in the thermal centre; (x) water bath.

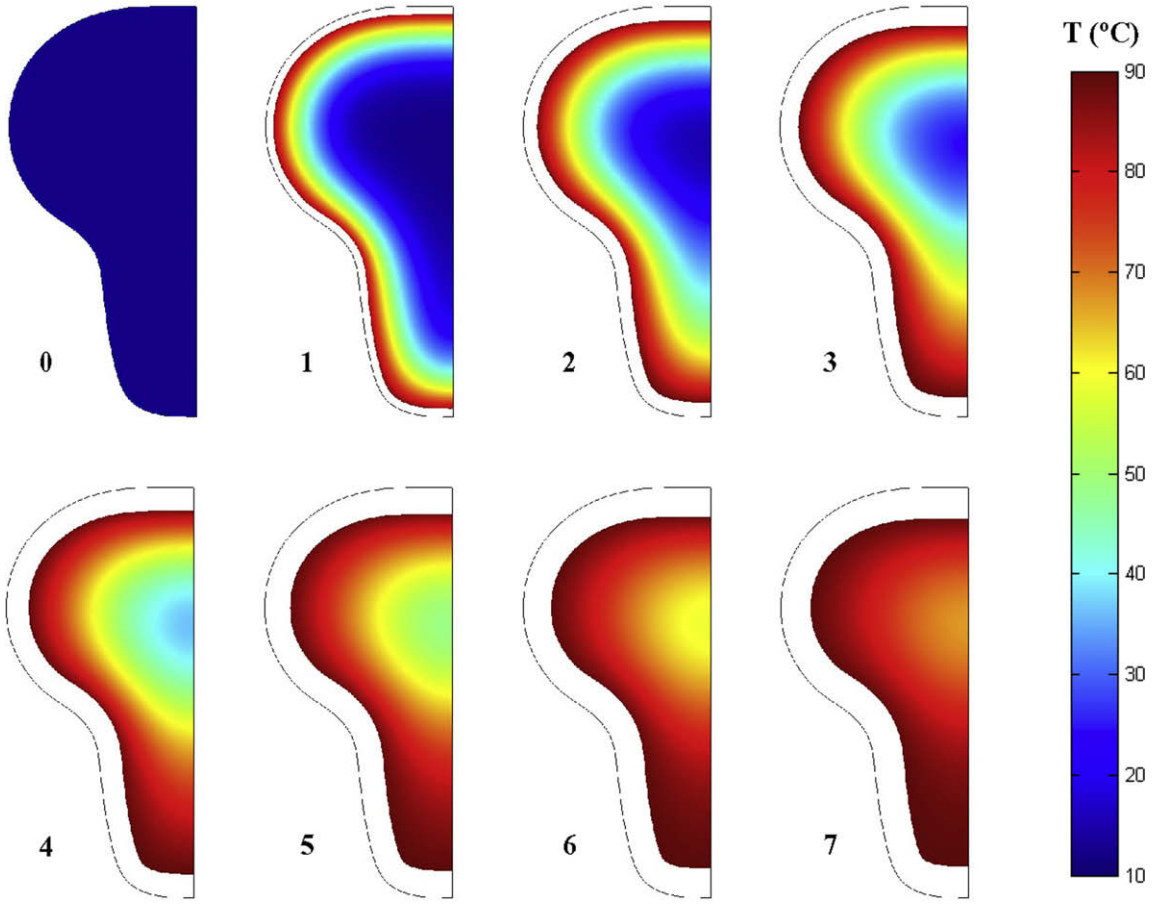

Fig. 9. Sequence of simulated images using the 2D axisymmetric geometry, at 30 s intervals, showing temperature distribution and size contraction during blanching at 90 °C. (For interpretation to colours in this figure, the reader is referred to the web version of this paper.)

than 4.19% were found between predicted and experimental temperatures for all the tests.

Simulated temperatures for the thermal centre showed a higher delay than those experimental ones. This phenomenon can be owed to the high differences in thermal conductivity (k) and specific heat (C_p) between thermocouple and mushroom, as was previously described by Akterian (1995).

Fig. 9 shows predicted temperature distribution and size variation in the mushroom, every one minute, during blanching at 90 °C, obtained using an axisymmetric two-dimensional geometry. During the first minutes of heating, a marked difference in temperatures appeared between surface and the inner parts of the vegetable. This difference decreased and tended to disappear as heating time advanced. Simultaneously, at the initial stage, mushroom size decreases rapidly, lowering shrinking rate towards the end of the process, as experimentally assessed previously. Similar behaviours for temperature variation and size reduction were obtained for the other process conditions.

Temperature profiles in Fig. 10 display the simulated temperature evolution during blanching at 50 °C and 90 °C along a horizontal line perpendicular to the thermal centre (Fig. 10a and b, respectively). It can be seen that at low bath temperature (Fig. 10a), mushrooms exhibited a less marked temperature profile, tending to an uniform temperature distribution at the end of the process; on the contrary, significant differences were predicted for high bath temperatures (Fig. 10b). These temperature differences induce important variations in cooking values for both regions (cap and stem) for high-temperature blanching processes.

Concerning mushrooms it is worth to remark that the two and three-dimensional domain simulations are absolutely equivalent from the point of view of sample shape and heat transfer conditions. Eventual slight differences in predicted values arise from the use of different meshes. However the calculation (running) time of two-dimensional domains were much lower than those of three-dimensional ones (9.38 s and 1401.38 s, respectively, for the same run).

4.3. Cooking value

Simulated average C_{ave} and surface C_{sur} cooking values are shown in Fig. 11. C_{ave} presented the highest value at intermediate heating temperatures (near 80 °C). Also, the difference between

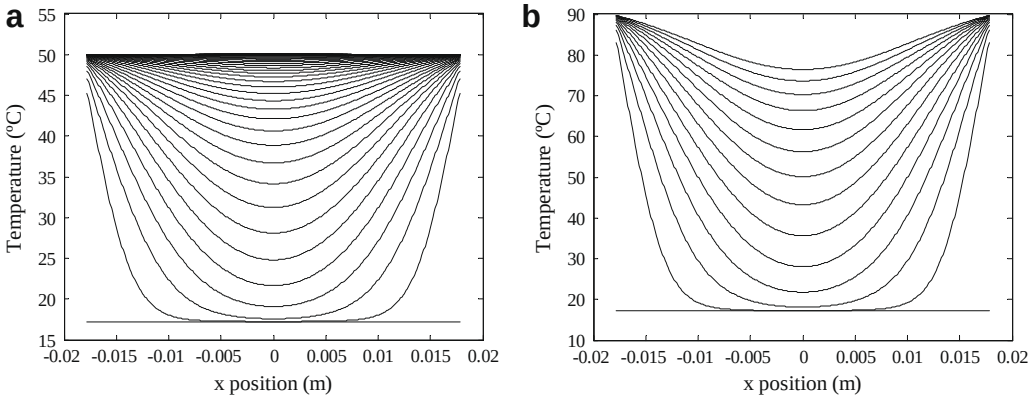

Fig. 10. Temperature profiles along the x-axis at 30-second intervals, for different water bath temperatures. (a) 50 °C, 77 min; (b) 90 °C, 7 min.

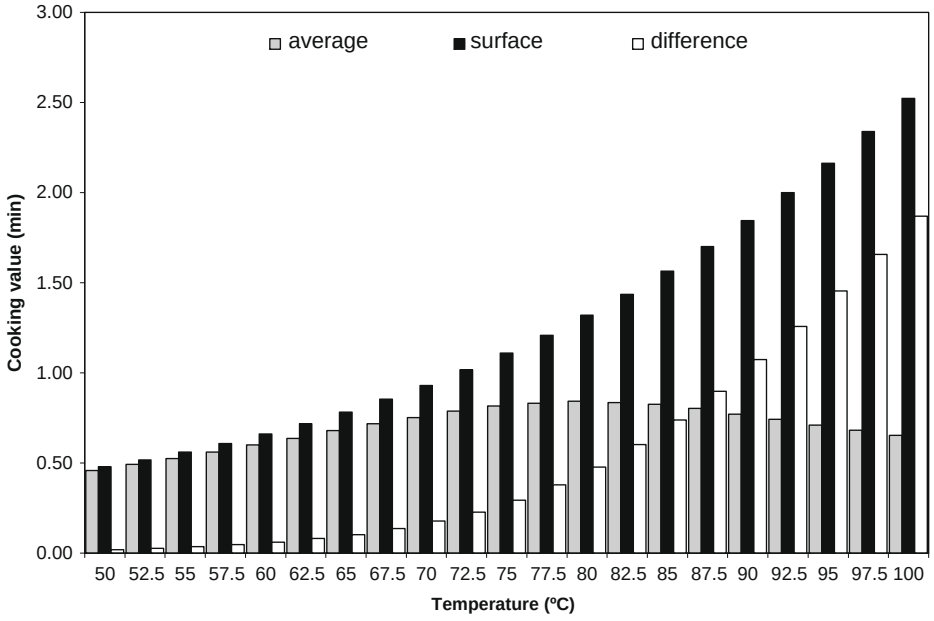

Fig. 11. Surface (C_{sur}), average (C_{ave}) and difference of cooking values, simulated for several process temperatures between 50 and 100 °C.

both cooking values increased with bath temperature. These differences were in accordance with the temperature profiles shown previously (Fig. 10). C_{sur} continuously augmented with processing temperature due that surface quickly reaches bath temperature and then remain constant during processing.

4.4. Texture

Important texture losses – in terms of maximum force (N) –, in the range of 64.18–80.28%, were determined after the different blanching processes. These values are similar to those reported by Matser et al. (2000) for mushrooms blanched during 5 min in boiling water. These authors determined a loss in stiffness in the order of 90%. Although no statistically significant differences were determined among the tested process conditions (Fig. 12), the highest texture loss was measured at intermediate temperatures, which was closely related to the predicted cooking values. Both quality indexes may follow similar variation kinetics.

4.5. Colour and Polyphenoloxidase enzymatic activity

In fresh samples, the values of parameters L^*, a^*, and b^* were 85.4, 1.06 and 16.71, respectively, similarly to those determined by Matser et al. (2000). Unprocessed mushrooms documented an enzymatic activity of 0.0766 ΔDO min^{-1} g^{-1}.

The three colour parameters varied during blanching, under all the tested heating conditions (see Table 3). Lightness (L^*) lowered,

Table 3
Relative percent variation of parameters L^*, a^*, and b^* with blanching temperature.

Temperature (°C)	L^* (%)	a^* (%)	b^* (%)
50	−38.52	423.78	1.40
60	−27.04	381.56	11.64
70	−16.29	96.22	19.29
80	−12.09	36.55	17.65
90	−3.30	13.12	22.73

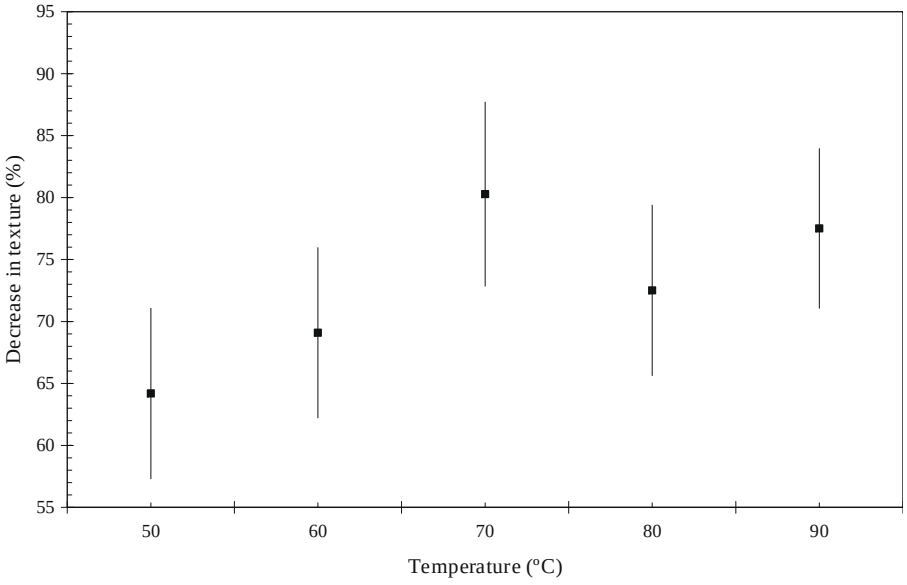

Fig. 12. Relative percent loss of texture after blanching at different temperatures.

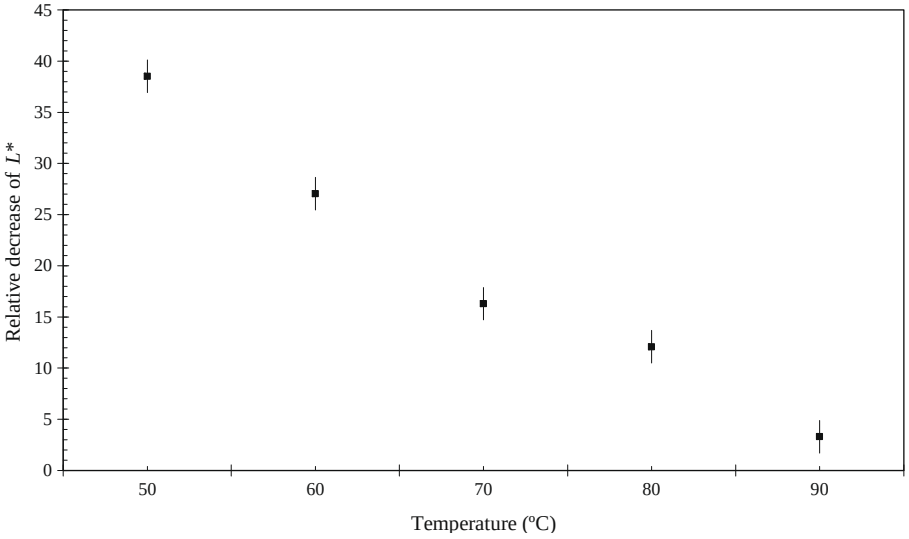

Fig. 13. Relative percent decrease of lightness after blanching at different temperatures.

showing darkening, meanwhile a^* and b^* increased indicating browning. Lightness reduction declined linearly whereas water bath temperature increased (Fig. 13).

Mushrooms blanched at 60, 70, 80 and 90 °C suffered total enzyme inactivation (at the estimated process time), meanwhile enzyme was partially inactivated ($0.0186\ \Delta DO\ min^{-1}\ g^{-1}$) when mushrooms were heated at 50 °C. These results coincide with those reported by McCord and Kilara (1983) who concluded that PPO was unaffected at temperatures lower than 45 °C, meanwhile at a blanching temperature of 50 °C a process time higher than 35.83 min was essential to lower enzymatic activity to 50% of its original value.

The different degrees of browning (stronger browning at lower bath temperatures) can be explained because at low temperatures (50 °C) enzymes remain active during most part of the blanching period. As the bath temperature increases (60–80 °C), the enzyme remains active for less time, producing smaller quantities of coloured products. Meanwhile at higher temperatures (90 °C) their inactivation is almost instantaneous, and there are almost no coloured products of enzymatic browning.

5. Conclusions

The developed simple shrinkage kinetic model of mushroom during blanching allows a quick estimation of the processing time needed to obtain a desirable size reduction. Furthermore, considering that several factors should be achieved during blanching, shrinkage appears to be the limiting factor controlling the needed processing time, at blanching temperatures above 60 °C, since no PPO activity is detected. When lower blanching temperatures are used the PPO activity reduction appears to be the slower process, and then controlling the processing time.

On the other hand under each process condition marked reductions were observed concerning lightness and texture. Also, it was noted that the reductions of these parameters were different for each treatment. This means that the blanching process could be optimized by selecting the most appropriated conditions.

Shrinkage and heat transfer model coupling allow obtaining good temperature predictions. Thus, cooking value can be estimated and correlated with quality index variations.

Acknowledgments

Authors acknowledge the financial support of CONICET, UNLP and ANPCyT from Argentina.

References

Akterian, S.G., 1995. Numerical simulation of unsteady heat transfer in canned mushrooms in brine during sterilization processes. Journal of Food Engineering 25 (1), 45–53.

Biekman, E.S.A., Kroese-Hoedeman, H.I., Schijvens, E.P.H.M., 1996. Loss of solutes during blanching of mushrooms (*Agaricus bisporus*) as a result of shrinkage and extraction. Journal of Food Engineering 28 (2), 139–152.

Biekman, E.S.A., van Remmen, H.H.J., Kroese-Hoedeman, H.I., Ogink, J.J.M., Schijvens, E.P.H.M., 1997. Effect of shrinkage on the temperature increase in evacuated mushrooms (*Agaricus bisporus*) during blanching. Journal of Food Engineering 33 (1–2), 87–99.

CIE (1978). Recommendations on uniform colour spaces – colour difference equations, psychometric colour terms. Supplement No. 2. CIE Publication No. 15(E-1-3.1) 1971/(TC-1-3). Paris: CIE.

COMSOL, AB (2005). COMSOL Multiphysics user's guide. Version: September 2005, COMSOL 3.2.

Concellón, A. (2003). Daño por frío en frutos no-climatéricos. PhD Thesis, Universidad Nacional de La Plata, La Plata, Argentina.

Devece, C., Rodríguez-López, J.N., Fenoll, J.T., Catalá, J.M., De los Reyes, E., García-Cánovas, F., 1999. Enzyme inactivation analysis for industrial blanching applications: comparison of microwave, conventional, and combination heat treatments on mushroom polyphenoloxidase activity. Journal of Agricultural and Food Chemistry 47 (11), 4506–4511.

Goñi, S.M., Purlis, E., Salvadori, V.O., 2007. Three-dimensional reconstruction of irregular foodstuffs. Journal of Food Engineering 82 (4), 536–547.

Konanayakam, M., Sastry, S.K., 1988. Kinetics of shrinkage of mushroom during blanching. Journal of Food Science 53 (5), 1406–1411.

Kotwaliwale, N., Bakane, P., Verma, A., 2007. Changes in textural and optical properties of oyster mushroom during hot air drying. Journal of Food Engineering 78 (4), 1207–1211.

Matser, A.M., Knott, E.R., Teunissen, P.G.M., Bartels, P.V., 2000. Effects of high isostatic pressure on mushrooms. Journal of Food Engineering 45 (1), 11–16.

McArdle, F.J., Curwen, D., 1962. Some factors influencing shrinkage of canned mushrooms. Mushroom Science 5, 547–557.

McCord, J.D., Kilara, A., 1983. Control of enzymatic browning in processed mushrooms (*Agaricus bisporus*). Journal of Food Science 48 (6), 1479–1483.

Ohlsson, T., 1980. Temperature dependence of sensory quality changes during thermal processing. Journal of Food Science 45 (4), 836–847.

Sastry, S.K., Beelman, R.B., Speroni, J.J., 1985. A three-dimensional finite element model for thermally induced changes in foods: Application to degradation of agaritine in canned mushrooms. Journal of Food Science 50 (5), 1293–1299.

Sensoy, I., Sastry, S.K., 2004. Ohmic blanching of mushrooms. Journal of Food Process Engineering 27 (1), 1–15.

Sheen, S., Hayakawa, K., 1991. Finite difference simulation for heat conduction with phase change in an irregular food domain with volumetric change. International Journal of Heat and Mass Transfer 34 (6), 1337–1346.